ChemComm

COMMUNICATION

Cite this: *Chem. Commun.*, 2021, **57**, 2551

Received 15th December 2020,
Accepted 1st February 2021

DOI: 10.1039/d0cc08128k

rsc.li/chemcomm

New up-conversion luminescence in molecular cyano-substituted naphthylsalophen lanthanide(III) complexes†

Jorge H. S. K. Monteiro, ‡[a] Ethan A. Hiti,[b] Emily E. Hardy,§[b] Grant R. Wilkinson,[b] John D. Gorden,[bc] Anne E. V. Gorden *[bc] and Ana de Bettencourt-Dias *[a]

A new naphthylsalophen and its 3:2 ligand-to-lanthanide sandwich-type complexes were isolated. When excited at 380 nm, the complexes display the characteristic metal-centred emission for Nd^{III}, Er^{III} and Yb^{III}. Upon 980 nm excitation, in mixed lanthanide and the Er complexes, Er-centred upconversion emission at 543 and 656 nm is observed, with power densities as low as 2.18 W cm^{-2}.

The unique luminescence properties of lanthanide (Ln^{III}) ions make their complexes interesting for a variety of applications.[1–3] These properties include colour purity, due to the core nature of the f orbitals involved in the emission process, and long luminescence lifetimes, due to the electronic-dipole forbidden nature of the f–f transitions, which enable time-delayed emission spectroscopy with increased signal-to-noise ratio.[4–6] The forbidden nature of these transitions makes sensitization of the emission more efficiently achieved through coordinated ligands in a process called the antenna effect.[4–6]

For low energy sensitization, excitation can be achieved through non-linear optical processes, such as two-photon absorption or cumulative effects of multiple first-order absorption phenomena, namely up-conversion (UC). The latter can occur through either excited-state absorption (ESA) or energy transfer up-conversion (ETU) (Fig. 1a).[7] The presence of spin allowed transitions in ions like Yb^{III} and Er^{III} results in a high absorption cross-section, and long-lived intermediate excited states enable the use of inexpensive and low power continuous-wave lasers to access them.[8] In ETU, a sensitizer ion absorbs low-energy photons, followed by energy transfer (ET) to the activator ion, which then emits in a characteristic wavelength. Er^{III} and Yb^{III}-doped nanoparticles (NPs) are among the most efficient UC systems.[9,10] The resonance between the excited states of Yb^{III} ($^4F_{5/2}$, ~10 624 cm^{-1}) and Er^{III} ($^4I_{11/2}$, ~10 346 cm^{-1}) improves the ET rates, and thus contributes to high UC emission intensities. While these NPs find wide application in bioimaging,[11–14] as they can be excited in a region of the spectrum where tissues have low absorption,[15,16] controlling their size, low cell penetrability, undesirable accumulation in the body, and stabilizing the crystalline phase that yields the highest UC luminesce intensity, such as the β-phase of $NaYF_4$,[17,18] are challenges for their use *in vivo*.[19,20]

In contrast, in Ln^{III} complexes toxicity and low cell penetrability are not inherent and emission properties do not depend on the crystalline phase. In addition, judiciously designed ligands allow tuning of solubility, biocompatibility, and photophysics of the complexes, among other properties.[21–23]

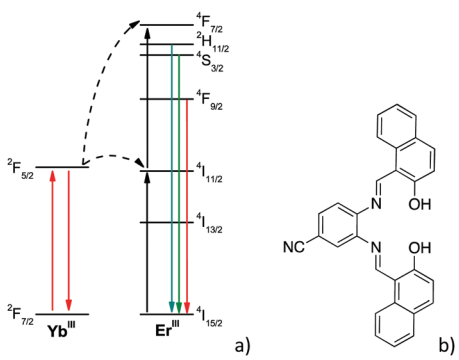

Fig. 1 (a) Energy level diagram illustrating the up-conversion process through ESA (two black up-arrows on Er^{III}) and ETU (dashed arrows, red up-arrow on Yb^{III} followed by top black up-arrow on Er^{III}). (b) Structure of H_2L-CN.

[a] *Department of Chemistry, University of Nevada, Reno, Nevada 89557, USA. E-mail: abd@unr.edu*

[b] *Department of Chemistry and Biochemistry, Auburn University, Auburn, Alabama 36849, USA*

[c] *Department of Chemistry and Biochemistry, Texas Tech University, Lubbock, Texas 79409, USA*

† Electronic supplementary information (ESI) available: Crystallographic details, syntheses, spectroscopic and spectrometric characterization. CCDC 1964321 and 1964323. For ESI and crystallographic data in CIF or other electronic format see DOI: 10.1039/d0cc08128k

‡ Current address: Department of Chemistry, Humboldt State University, Arcata, CA 95521, USA.

§ Current address: Department of Chemistry, Old Dominion University, Norfolk, VA 23529, USA.

UC is important in bioimaging and sensing applications, and there is substantial interest in small-molecule probes,[24,25] yet examples using Ln^{III} complexes are less common than those of Ln–$NaYF_4$-based NPs. The lattice on the latter is a low-phonon system, which is necessary for good UC efficiency.[26] Piguet and co-workers pioneered the UC luminescence using Ln^{III} complexes.[27] Charbonnière and co-workers demonstrated UC luminescence in deuterated water in a dimeric Er^{III} complex, in which this ion is both activator and sensitizer.[28] Hyppänen and co-workers[29] and more recently, Piguet and co-workers demonstrated that mononuclear Er^{III} complexes are capable of showing UC luminescence.[30] Many of the known examples have low UC emission intensity despite deuteration of the ligand, or require a transition metal as sensitizer or use metalorganic frameworks to reduce vibrational quenching; others, due to the long distances between the metal ions, require high excitation laser power densities to increase the ET efficiency.[31–35] Thus, the isolation of efficient Ln^{III}-based UC molecules is a current challenge.[36,37]

Recently, Gorden and co-workers showed that naphthylsalophen ligands form Ln^{III} complexes with a rigid sandwich structure in a 2:3 (Ln^{III}:ligand) stoichiometry.[38] Because the Ln^{III}–Ln^{III} distance in these compounds is in the range 3.768–4.016 Å, well within the range for optimal Förster ET,[7,39] these structures are good candidates for UC luminescence. Therefore, to increase our knowledge of ligand and complex architectures that enable UC properties in Ln^{III}-based molecular systems, we synthesized mixed Er^{III}, Yb^{III} and pure Er^{III} complexes containing a new naphthylsalophen ligand with the cyano-electron-withdrawing group in the backbone. These compounds indeed display UC luminescence, as described below, adding new examples to a small group of molecular Ln^{III} complexes that exhibit this property.

The protonated cyano-naphthylsalophen H_2L-CN (Fig. 1b) is isolated by condensation of 3,4-diaminobenzonitrile with 2-hydroxynaphthaldehyde in EtOH. The Ln^{III} complexes (Gd^{III}, Nd^{III}, Er^{III}, and Yb^{III}) are prepared by addition of the Ln^{III} metal salt, either the chloride or the acetate, in MeOH to the ligand in THF and of triethylamine (TEA) to deprotonate the ligand.

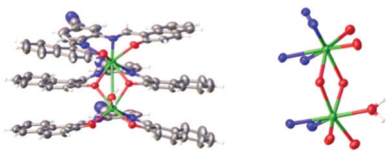

Fig. 2 Left: Projection of the front view of $[Er_2(L\text{-}CN)_3(H_2O)]$. Right: Coordination environments of Er1 (bottom) and Er2 (top). Carbon atoms are shown in grey, nitrogen in blue, oxygen in red, and erbium in green.

X-ray quality crystals of H_2L-CN indicate that the compound crystalizes in the space group $P21/c$ (Fig. S18, ESI†) and does not display interactions with solvent molecules of crystallization.

The structure of $[Er_2(L\text{-}CN)_3(H_2O)]$ (Fig. 2 and Fig. S19, ESI†) shows features similar to previously reported Ln^{III} triple decker complexes.[38] The Er2 metal centre is 8-coordinate and the coordination sphere is completed by the ligand, while the Er1 metal centre is seven-coordinate, bound to ligand and one water molecule (Fig. 2 right). The distance between metal centres is 3.816 Å, within the Förster ET range.[7,39]

Deconvolution of the fluorescence and phosphorescence spectra of the Gd^{III} complexes (Fig. S14, ESI†) into the vibrational components yields energies at ~18 400 and ~15 900 cm^{-1} for the excited singlet and triplet levels, respectively (Fig. S14(b and c), ESI†). The triplet energy level is suitably located to sensitize the NIR-emitting Ln^{III} (Nd^{III}, Yb^{III} and Er^{III}), as shown in Fig. S15 (ESI†). The one-photon solution excitation and emission spectra of Nd^{III}, Yb^{III} and Er^{III} complexes in dichloromethane are shown in Fig. S16 (ESI†). The excitation spectra of the complexes are composed of broad bands, consistent with sensitization of Ln^{III} emission through the ligand, as indicated by the overlap of excitation and absorption spectra shown, representatively, for the Yb^{III} complex in Fig. S16 (ESI†). The emission spectrum of the Nd^{III} complex shows the expected $^4F_{3/2} \rightarrow {}^4I_J$ (J = 9/2–13/2) transitions. For the Yb^{III} complex the $^2F_{5/2} \rightarrow {}^2F_{7/2}$ transitions, and for the Er^{III} complex the $^4I_{13/2} \rightarrow {}^4I_{15/2}$ transitions are observed. The quantum yields of sensitized emission (Φ_L^{Ln}) for the Nd^{III} and Yb^{III} complexes are summarized in Table 1. They are comparable with reported values for other complexes of these ions.[40–42] The emission lifetimes of the Yb^{III} complexes, summarized in Table 1, are comparable as well with values reported for this ion.[41,43,44] The excited state decay curves were fitted to a bi-exponential, consistent with the presence of ions in two different coordination environments (Fig. S17, ESI†). We attribute the shortest lifetime to the Yb^{III} site with a coordinated solvent molecule, and the longest one to the Yb^{III} bound only to ligand.

We isolated multi-Ln^{III} complexes by adapting the procedure described for the homonuclear complexes. Y^{III} as diluting ion, Yb^{III} and Er^{III}, or Yb^{III} and Er^{III} were added to a solution of the

Table 1 Singlet ^1S and triplet ^3T state energies of the ligands, excited state lifetime τ, and quantum yield Φ_L^{Ln} of sensitized efficiency for the Nd^{III}, Yb^{III} and Er^{III} complexes. λ_{exc} = 380 nm and [complex] = 1×10^{-4} M

Complexes	Solvent	$^1S^a$ [cm^{-1}]	$^3T^a$ [cm^{-1}]	τ^b [μs]	Φ_L^{Ln} [%]
$[Nd_2(L\text{-}CN)_3(H_2O)]$	CH_2Cl_2	18 420 ± 70	15 910 ± 50	[c]	0.0054 ± 0.0009
$[Yb_2(L\text{-}CN)_3(H_2O)]$				1.230 ± 0.027 (81.1) 6.801 ± 0.197 (18.9)	0.154 ± 0.013
$[Er_2(L\text{-}CN)_3(H_2O)]$				[c]	[c]

[a] Determined at 77 K, using the analogous Gd complexes.[47] [b] The values in parenthesis indicate the percent contribution of each lifetime. [c] Too weak to be quantified.

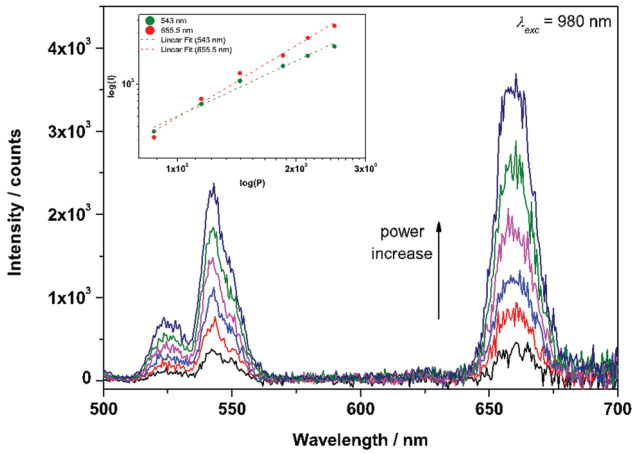

Fig. 3 Two-photon UC emission spectra of $[(Y_{0.76}Yb_{0.16}Er_{0.08})_2(L\text{-}CN)_3(H_2O)]$ in the solid state using variable laser power. Inset shows plot of the log of the emission intensity I at 543 nm (green dots) or 655.5 nm (red dots) as a function of the log of the laser power P. λ_{exc} = 980 nm, P = 0.873–2.500 W.

deprotonated ligand in 2 : 3 (Ln : L) molar ratio. The $[(Y_{0.76}Yb_{0.16}Er_{0.08})_2(L\text{-}CN)_3(H_2O)]$ complex, with metal stoichiometry determined through energy-dispersive X-ray spectroscopy (EDS), can be excited in the solid state by two low energy photons through an UC process.[7] The resulting spectrum (Fig. 3) shows Er^{III}-centred transitions in the green ($^2H_{11/2} \rightarrow {}^4I_{15/2}$ and $^4S_{3/2} \rightarrow {}^4I_{15/2}$) and red ($^4I_{9/2} \rightarrow {}^4I_{15/2}$) upon excitation at 980 nm. The quadratic dependence of the emission intensity (I) on the laser power (P) (inset of Fig. 3) confirms the 2-photon nature of the process (data in Table S1, ESI†). UC emission is observed for power densities as low as 2.18 W cm^{-2}, which compares favourably with known efficient systems (29 W cm^{-2}).[28,30,31,45]

Emission following UC excitation is also observed for $[(Yb_{0.78}Er_{0.22})_2(L\text{-}CN)_3(H_2O)]$ and $[Er_2(L\text{-}CN)_3(H_2O)]$ (Fig. 4, top and bottom traces, respectively) in the solid state. Although there is an increase of the emission intensity for $[(Yb_{0.78}Er_{0.22})_2(L\text{-}CN)_3(H_2O)]$ as compared with the trimetallic complex, the concentration of Er^{III} is 4.7-fold higher in the former. In $[(Yb_{0.78}Er_{0.22})_2(L\text{-}CN)_3(H_2O)]$ and $[Er_2(L\text{-}CN)_3(H_2O)]$ UC emission was observed with power densities as low as 2.18 W cm^{-2} and 6.25 W cm^{-2}, respectively. The UC emission intensity of the latter is lower, due to non-radiative cross-relaxation.[46] The complexes did not show upconversion when dissolved in acetonitrile, chloroform and deuterated chloroform.

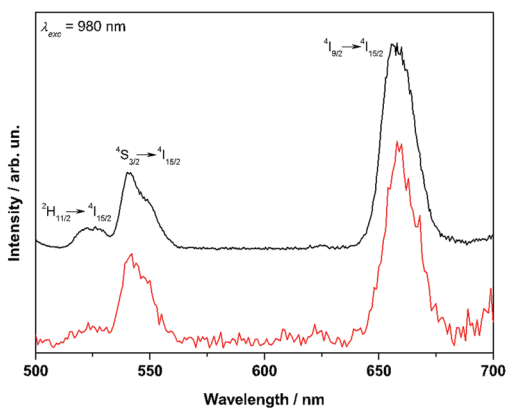

Fig. 4 Two-photon UC emission spectra of $[(Yb_{0.78}Er_{0.22})_2(L\text{-}CN)_3(H_2O)]$ (black upper trace) and $[Er_2(L\text{-}CN)_3(H_2O)]$ (red bottom trace) in the solid state. λ_{exc} = 980 nm, P = 2.5 W.

In conclusion, we isolated three Ln^{III} complexes with a cyano-naphthylsalophen ligand with a 2 : 3 stoichiometry and sandwich structure. These complexes display efficient one-photon Nd^{III}- and Yb^{III}-centred emission and weak Er^{III}-centred emission.

Complexes containing a mixture of Er^{III} and Yb^{III}, or Er^{III}, Yb^{III} and Y^{III} or just Er^{III} also display Er-centred red and green emission upon excitation with a 980 nm laser at low power densities, indicative of UC, making these systems rare examples of upconverting Ln^{III}-based molecules. This work increases our knowledge of molecular complexes of Ln^{III} ions that can be excited at low energy with a low intensity laser and are thus of potential interest for biological imaging applications.

Author contributions: JHSKM performed the one- and two-photon characterization of the complexes, EAH synthesized ligand and metal complexes and performed solution characterization, EEH initially synthesized the ligand, GRW contributed to synthesis and solution characterization, JDG did X-ray crystallographic characterization. Experimental work and manuscript preparation were supervised by AEVG and AdBD.

Financial support of this work is gratefully acknowledged (NSF CHE-1800392 to AdBD and DOE-BES CSGB DE-SC0019177 to AEVG).

Conflicts of interest

There are no conflicts to declare.

References

1 J.-C. G. Bünzli, Lanthanide luminescence for biomedical analyses and imaging, *Chem. Rev.*, 2010, **110**, 2729–2755.
2 J. Zhao, J. Gao, W. Xue, Z. Di, H. Xing, Y. Lu and L. Li, Upconversion Luminescence-Activated DNA Nanodevice for ATP Sensing in Living Cells, *J. Am. Chem. Soc.*, 2018, **140**, 578–581.
3 J. Hai, T. Li, J. Su, W. Liu, Y. Ju, B. Wang and Y. Hou, Anions Reversibly Responsive Luminescent Tb(III) Nanocellulose Complex Hydrogels for Latent Fingerprint Detection and Encryption, *Angew. Chem., Int. Ed.*, 2018, **57**, 6786–6790.
4 J.-C. G. Bünzli, On the design of highly luminescent lanthanide complexes, *Coord. Chem. Rev.*, 2015, **293–294**, 19–47.
5 A. de Bettencourt-Dias, Introduction to Lanthanide Ion Luminescence, in *Luminescence of Lanthanide Ions in Coordination Compounds and Nanomaterials*, ed. A. de Bettencourt-Dias, Wiley, 2014.
6 J.-C. G. Bünzli and C. Piguet, Taking advantage of luminescent lanthanide ions, *Chem. Soc. Rev.*, 2005, **34**, 1048–1077.
7 F. Auzel, Upconversion and Anti-Stokes Processes with f and d Ions in Solids, *Chem. Rev.*, 2004, **104**, 139–173.
8 C. Chen, F. Wang, S. Wen, Q. P. Su, M. C. L. Wu, Y. Liu, B. Wang, D. Li, X. Shan, M. Kianinia, I. Aharonovich, M. Toth, S. P. Jackson, P. Xi and D. Jin, Multi-photon near-infrared emission saturation nanoscopy using upconversion nanoparticles, *Nat. Commun.*, 2018, **9**, 3290.

9 J. Zhou, Q. Liu, W. Feng, Y. Sun and F. Li, Upconversion Luminescent Materials: Advances and Applications, *Chem. Rev.*, 2015, **115**, 395–465.
10 E. K. Lim, T. Kim, S. Paik, S. Haam, Y. M. Huh and K. Lee, Nanomaterials for Theranostics: Recent Advances and Future Challenges, *Chem. Rev.*, 2015, **115**, 327–394.
11 G. Y. Chen, H. L. Qju, P. N. Prasad and X. Y. Chen, Upconversion Nanoparticles: Design, Nanochemistry, and Applications in Theranostics, *Chem. Rev.*, 2014, **114**, 5161–5214.
12 O. S. Wolfbeis, An overview of nanoparticles commonly used in fluorescent bioimaging, *Chem. Soc. Rev.*, 2015, **44**, 4743–4768.
13 G. Liu, F. Jiang, Y. Chen, C. Yu, B. Ding, S. Shao, M. Jia, P. a. Ma, Z. Fu and J. Lin, Superior temperature sensing of small-sized upconversion nanocrystals for simultaneous bioimaging and enhanced synergetic therapy, *Nanomedicine*, 2019, **24**, 102135.
14 D. J. Gargas, E. M. Chan, A. D. Ostrowski, S. Aloni, M. V. P. Altoe, E. S. Barnard, B. Sanii, J. J. Urban, D. J. Milliron, B. E. Cohen and P. J. Schuck, Engineering bright sub-10-nm upconverting nanocrystals for single-molecule imaging, *Nat. Nanotechnol.*, 2014, **9**, 300–305.
15 C.-F. Chan, M.-K. Tsang, H. Li, R. Lan, F. L. Chadbourne, W.-L. Chan, G.-L. Law, S. L. Cobb, J. Hao, W.-T. Wong and K.-L. Wong, Bifunctional up-converting lanthanide nanoparticles for selective in vitro imaging and inhibition of cyclin D as anticancer agents, *J. Mater. Chem. B*, 2014, **2**, 84.
16 M. Jiang, H. Liu, S. Zeng and J. Hao, A General In Situ Growth Strategy of Designing Theranostic NaLnF4@Cu_{2-x}S Nanoplatform for In Vivo NIR-II Optical Imaging Beyond 1500 nm and Photothermal Therapy, *Adv. Ther.*, 2019, **2**, 1800153.
17 M. Zhao, B. Li, P. Wang, L. Lu, Z. Zhang, L. Liu, S. Wang, D. Li, R. Wang and F. Zhang, Supramolecularly Engineered NIR-II and Upconversion Nanoparticles In Vivo Assembly and Disassembly to Improve Bioimaging, *Adv. Mater.*, 2018, **30**, 1804982.
18 D. Li, S. He, Y. Wu, J. Liu, Q. Liu, B. Chang, Q. Zhang, Z. Xiang, Y. Yuan, C. Jian, A. Yu and Z. Cheng, Excretable Lanthanide Nanoparticle for Biomedical Imaging and Surgical Navigation in the Second Near-Infrared Window, *Adv. Sci.*, 2019, **6**, 1902042.
19 S. K. Nune, P. Gunda, P. K. Thallapally, Y.-Y. Lin, M. Laird Forrest and C. J. Berkland, Nanoparticles for biomedical imaging, *Expert Opin. Drug Delivery*, 2009, **6**, 1175–1194.
20 Y.-W. Huang, M. Cambre and H.-J. Lee, The Toxicity of Nanoparticles Depends on Multiple Molecular and Physicochemical Mechanisms, *Int. J. Mol. Sci.*, 2017, **18**, 2702.
21 C. L. Wagner, L. Tao, J. C. Fettinger, R. D. Britt and P. P. Power, Two-Coordinate, Late First-Row Transition Metal Amido Derivatives of the Bulky Ligand -N(SiPri3)Dipp (Dipp = 2,6-diisopropylphenyl): Effects of the Ligand on the Stability of Two-Coordinate Copper(II) Complexes, *Inorg. Chem.*, 2019, **58**, 8793–8799.
22 A. C. Brannan and Y. Lee, Photophysical tuning of s-SiH coppercarbazolide complexes to give deep-blue emission, *Inorg. Chem.*, 2020, **59**, 315–324.
23 T. Sherstobitova, K. Maryunina, S. Tolstikov, G. Letyagin, G. Romanenko, S. Nishihara and K. Inoue, Ligand Structure Effects on Molecular Assembly and Magnetic Properties of Copper(II) Complexes with 3-Pyridyl-Substituted Nitronyl Nitroxide Derivatives, *ACS Omega*, 2019, **4**, 17160–17170.
24 H. M. Kim and B. R. Cho, Small-Molecule Two-Photon Probes for Bioimaging Applications, *Chem. Rev.*, 2015, **115**, 5014–5055.
25 L. Qian, L. Li and S. Q. Yao, Two-Photon Small Molecule Enzymatic Probes, *Acc. Chem. Res.*, 2016, **49**, 626–634.
26 G. Liu, Advances in the theoretical understanding of photon upconversion in rare-earth activated nanophosphors, *Chem. Soc. Rev.*, 2015, **44**, 1635–1652.
27 L. Aboshyan-Sorgho, C. Besnard, P. Pattison, K. R. Kittilstved, A. Aebischer, J.-C. G. Bünzli, A. Hauser and C. Piguet, Near-Infrared → Visible Light Upconversion in a Molecular Trinuclear d–f–d Complex, *Angew. Chem., Int. Ed.*, 2011, **50**, 4108–4112.
28 A. Nonat, C. F. Chan, T. Liu, C. Platas-Iglesias, Z. Liu, W.-T. Wong, W.-K. Wong, K.-L. Wong and L. J. Charbonnière, Room temperature molecular up conversion in solution, *Nat. Commun.*, 2016, **7**, 11978.
29 I. Hyppännen, S. Lahtinen, T. Ääritalo, J. Mäkelä, J. Kankare and T. Soukka, Photon Upconversion in a Molecular Lanthanide Complex in Anhydrous Solution at Room Temperature, *ACS Photonics*, 2014, **1**, 394–397.
30 B. Golesorkhi, H. Nozary, L. Guénée, A. Fürstenberg and C. Piguet, Room-Temperature Linear Light Upconversion in a Mononuclear Erbium Molecular Complex, *Angew. Chem., Int. Ed.*, 2018, **57**, 15172–15176.
31 N. Souri, T. Tian, C. Platas-Iglesias, K.-L. Wong, A. Nonat and L. J. Charbonnière, Unconverted Photosensitization of Tb Visible Emission by NIR Yb Excitation in Discrete Supramolecular Heteropolynuclear Complexes, *J. Am. Chem. Soc.*, 2017, **139**, 1456–1459.
32 Y. Suffren, B. Golesorkhi, D. Zare, L. Guénée, H. Nozary, S. Eliseeva, S. Petoud, A. Hauser and C. Piguet, Taming Lanthanide-Centered Upconversion at the Molecular Level, *Inorg. Chem.*, 2016, **55**, 9964–9972.
33 M. Pollnau, D. R. Gamelin, S. R. Lüthi and H. U. Güdel, Power dependence of upconversion luminescence in lanthanide and transition-metal-ion systems, *Phys. Rev. B: Condens. Matter Mater. Phys.*, 2000, **61**, 3337–3346.
34 H. Ye, V. Bogdanov, S. Liu, S. Vajandar, T. Osipowicz, I. Hernández and Q. Xiong, Bright Photon Upconversion on Composite Organic Lanthanide Molecules through Localized Thermal Radiation, *J. Phys. Chem. Lett.*, 2017, **8**, 5695–5699.
35 J. Kalmbach, C. Wang, Y. You, C. Förster, H. Schubert, K. Heinze, U. Resch-Genger and M. Seitz, Near-IR to Near-IR Upconversion Luminescence in Molecular Chromium Ytterbium Salts, *Angew. Chem., Int. Ed.*, 2020, **59**, 18804–18808.
36 B. Golesorkhi, H. Nozary, A. Fürstenberg and C. Piguet, Erbium complexes as pioneers for implementing linear light-upconversion in molecules, *Mater. Horiz.*, 2020, **7**, 1279–1296.
37 A. M. Nonat and L. J. Charbonniere, Upconversion of light with molecular and supramolecular lanthanide complexes, *Coord. Chem. Rev.*, 2020, **409**, 213192.
38 E. E. Hardy, K. M. Wyss, R. J. Keller, J. D. Gorden and A. E. V. Gorden, Tunable ligand emission of napthylsalophen triple-decker dinuclear lanthanide(III) sandwich complexes, *Dalton Trans.*, 2018, **47**, 1337–1346.
39 P. Porcher and P. Caro, Crystal-field parameters for Eu^{3+} in KY_3F_{10}. III. Radiative and nonradiative transition probabilities, *J. Chem. Phys.*, 1978, **68**, 4183–4187.
40 A. de Bettencourt-Dias, P. S. Barber and S. Bauer, A water-soluble Pybox derivative and its highly luminescent lanthanide ion complexes, *J. Am. Chem. Soc.*, 2012, **134**, 6987–6994.
41 J. Zhang and S. Petoud, Azulene-moiety-based ligand for the efficient Sensitization of four near-infrared luminescent lanthanide cations: Nd^{3+}, Er^{3+}, Tm^{3+}, and Yb^{3+}, *Chem. – Eur. J.*, 2008, **14**, 1264–1272.
42 H. B. Wei, G. Yu, Z. F. Zhao, Z. W. Liu, Z. Q. Bian and C. H. Huang, Constructing lanthanide Nd(III), Er(III) and Yb(III) complexes using a tridentate N, N, O-ligand for near-infrared organic light-emitting diodes, *Dalton Trans.*, 2013, **42**, 8951–8960.
43 Y. Ning, Y.-W. Liu, Y.-S. Meng and J.-L. Zhang, Design of Near-Infrared Luminescent Lanthanide Complexes Sensitive to Environmental Stimulus through Rationally Tuning the Secondary Coordination Sphere, *Inorg. Chem.*, 2018, **57**, 1332–1341.
44 S. Shuvaev and D. Parker, A near-IR luminescent ratiometric ytterbium pH probe, *Dalton Trans.*, 2019, **48**, 4471–4473.
45 A. Nonat, S. Bahamyirou, A. Lecointre, F. Przybilla, Y. Mély, C. Platas-Iglesias, F. Camerel, O. Jeannin and L. J. Charbonnière, Molecular Upconversion in Heteropolynuclear Supramolecular Tb/Yb Assemblies, *J. Am. Chem. Soc.*, 2019, **141**, 1568–1576.
46 S. H. Wen, J. J. Zhou, K. Z. Zheng, A. Bednarkiewicz, X. G. Liu and D. Y. Jin, Advances in highly doped upconversion nanoparticles, *Nat. Commun.*, 2018, **9**, 2415.
47 G. A. Crosby, R. E. Whan and R. M. Alire, Intramolecular energy tranfer in rare earth chelates. Role of the triplet state, *J. Chem. Phys.*, 1961, **34**, 743–748.

